Tellus (2007), 59A, 384–394
Printed in Singapore. All rights reserved

TELLUS

A Study of the zonally asymmetric tropospheric forcing of the austral vortex splitting during September 2002

By DIETER PETERS[1]*, PAWEL VARGIN[2] and HEINER KÖRNICH[3] [1]*Leibniz-Institut für Atmosphärenphysik an der Universität Rostock e.V., Schlossstraße 6, D-18225 Ostseebad Kühlungsborn, Mecklenburg, Germany;* [2]*Central Aerological Observatory, Dolgoprudny, Moscow region, Russia;* [3]*Department of Meteorology, Stockholm University, Sweden*

(Manuscript received 15 March 2006; in final form 12 December 2006)

ABSTRACT

In September 2002, the first observed austral major warming was mainly characterized by a polar vortex splitting in the middle and upper stratosphere together with an ozone hole splitting. From our synoptic investigation based on ECMWF analyses, we establish the hypothesis that lower tropospheric processes at polar latitudes are primary responsible for the vortex splitting.

Over the coastline of Antarctica two regions occurred, one over the Ross shelf ice and the other over the Weddell shelf ice, where an enlarged tropospheric wave-activity generation in connection with an anticyclonic anomaly took place. The wave-activity flux was eastward and upward into the stratosphere, and was linked with an increasing ultra-long wave 2, which could be the primary reason for the vortex splitting in the stratosphere. In the troposphere, two Rossby wave trains have been identified which contribute mainly to the maintenance of the anticyclonic anomalies over both wave-activity generation regions.

1. Introduction

The first observed austral sudden major warming, in September 2002, was characterized by a strongly modulated polar vortex up to about 650 K – isentropic layer (∼27 km), and higher up by a vortex splitting into two vortices causing the splitting of the ozone hole (e.g. Baldwin et al., 2003; Simmons et al., 2003; Manney at al., 2005). The upper eastern vortex was stronger than the one over the western hemisphere, which moved equatorward and vanished later on. The eastern vortex moved poleward and re-established the polar vortex of the upper stratosphere in the middle of October, but broke down during the final warming before summer (e.g. Allen et al., 2003; Orsolini et al., 2005).

The splitting of the boreal polar vortex has been often reported (e.g. Labitzke and Naujokat, 2000), and is related to the "wave 2" type of warmings, whereas during the "wave 1" type the vortex is shifted out of the polar region. "Wave 2" type warmings of the so-called Berlin phenomenon (Scherhag, 1952) are much rarer than the "wave 1" type.

Especially, Charlton et al. (2005) presented a diagnostic overview of the evolution of the vortex splitting during September 2002, showing that the increasing stratospheric anticyclone in the Australasian sector played initially an important role in the splitting process. Nevertheless, they mentioned that two distinct cyclonic centres were present in the lower stratosphere at that time. For the set on of the major warming, they proposed an instability process (Plumb 1981) of the tropospheric–stratospheric system with a possible dynamical connection to the underlying topography, but the evolution is nonlinear.

This is in agreement with Krüger et al. (2005) who call the September 2002 major warming a typical wavenumber-1 warming because this wave dominated the change of the zonal flow and favoured the eastward propagation of a travelling wave 2.

Manney et al. (2005) concluded from their model study that anomalously strong tropospheric forcing (about 100 hPa) seems to be the primary direct cause of the austral major warming. In addition to wave 1 and 2 forcing, Manney et al. (2005) showed the important role of planetary wave 3 in the stratosphere in order to model the right position and intensity of both vortices during the splitting.

Based on NCEP/NCAR reanalysis project data, Nishii and Nakamura (2004; hereafter NN04) showed for austral mid-latitudes the direct tropospheric influence on the major warming event in late September 2002. They found an enlarged tropospheric forcing region of a Rossby wave packet (ultra-long wave 1 dominates and other harmonics are included) generating wave

*Corresponding author.
e-mail: peters@iap-korn.de
DOI: 10.1111/j.1600-0870.2007.00228.x

activity over the South Atlantic in connection with an anticyclone. From such a blocking ridge the enhanced wave activity propagates eastward and upward into the stratospheric polar night jet during the major warming. This mechanism with dominating wave 1 induced sudden warming was given by Matsuno (1971).

Furthermore, NN04 found that a wave train of quasi-stationary Rossby waves, starting in the South Pacific Convergence Zone some days earlier, contributes also to the maintenance of the quasi-stationary anticyclone over the South Atlantic in mid-latitudes.

The question of a direct tropospheric influence on the vortex splitting in the stratosphere during the major warming arises. If an amplified tropospheric Rossby wave 2 propagates upward into the stratosphere, it could support also a major warming with wave 1. Furthermore, if strong enough it splits the vortex into two vortices.

The aim of our investigation is to study the tropospheric influence on the major warming event and on the vortex splitting based on ECMWF analyses. We used nearly the same methods as NN04 but a different data set. Thereby, we confirm their results for mid-latitudes. However, by focusing the investigation on southern polar latitudes we found two regions of enhanced tropospheric wave activity generation which are related to two anticyclones in the troposphere and two cyclones in the lower stratosphere.

The intention of our article is to present diagnostic results, which support the hypothesis that tropospherically generated wave activity at two preferred regions over the coastline of Antarctica, propagated upward into the stratosphere and influenced the splitting of the south polar vortex into two vortices.

The methodology and data are described in Section 2, and results in Section 3, followed by a discussion in Section 4. Finally, the conclusions are presented in the last Section 5.

2. Methodology and data

This is a diagnostic study where we use some standard methods to analyse the zonally asymmetric forcing of quasi-stationary waves in the troposphere. We calculated the extended Eliassen–Palm (E–P) flux (Plumb 1985, hereafter P85) for quasi-stationary planetary waves, defined as composites of 5 d, in order to estimate the three-dimensional wave-activity flux vector $\underline{\mathrm{F}}$ and its divergence. Following Plumb (1985) and using standard notations we define $\underline{\mathrm{F}}$ for the deviations of meridional and zonal wind, geopotential and temperature from their zonal mean values with $f = 2\Omega \sin\varphi$, $d = 2\Omega a \sin(2\varphi)$ and S as stability:

$$\underline{F} = p\ p_S^{-1} \cos\varphi \begin{pmatrix} vv & - & d^{-1}\ \frac{\partial(v\phi)}{\partial\lambda} \\ -uv & + & d^{-1}\ \frac{\partial(u\phi)}{\partial\varphi} \\ vTfS^{-1} & - & fS^{-1}d^{-1}\ \frac{\partial(T\phi)}{\partial\lambda} \end{pmatrix} \tag{1}$$

Note, in diagnostic studies this flux vector is often employed for different time scales from climatological studies of wave-activity fluxes (e.g. P85) down to about 5 d composites studies (NN04).

The conservation relation for wave activity was derivated by using linear quasi-geostrophic theory of stationary planetary wave propagation in a zonal mean background stream (P85), and was successfully used to identify source and sink regions of wave activity by calculating the divergence and convergence of those fluxes. Plumb showed that in the WKB limit the wave-activity flux vector is proportional to the group velocity of a Rossby wave packet and it indicates the propagation direction of the wave activity from the troposphere into the stratosphere.

Furthermore, we use the Hovmöller diagram of squared meridional velocity to examine the evolution of wave packets as known from other studies (e.g. Chang 1993). This method was important in order to localize the group velocity of baroclinic waves in the tropophere, which contribute to the maintenance of blocking anticyclones. Additionally to NN04 we used the one-point correlation method (Bretherton et al., 1992) to identify wave trains starting their propagation from well-defined source regions. These source regions are differentiated by interpolated outgoing long-wave radiation (OLR from NOAA-CIRES) anomalies, vertical velocity distribution and an estimation of linear Rossby wave forcing about the tropopause (Sardeshmukh and Hoskins, 1988).

The data we used in this study are the ECMWF analyses based on a triangular (T512) spectral resolution. Then, the resolution was reduced to triangular T106, and grid values were estimated on a $1^\circ \times 1^\circ$ – latitude $\times$ longitude grid, a sufficient resolution for our purpose. The used daily data relates to 00 universal time values. However, for the one-point correlation maps with different time lags and for the calculations of vertical velocity and Rossby wave forcing we used six hourly values four times per day to improve the time resolution of those estimations.

3. Results

3.1. *Zonal mean evolution, E–P flux and wave amplitudes*

We start our analysis with a short overview on the zonal mean evolution of the zonal wind at 65° S and temperature at 80° S from August to October 2002 that means, zonal wind at the edge of the polar vortex and temperature near the centre of the polar vortex. In the middle and upper stratosphere, the zonal mean zonal wind (Fig. 1a) shows oscillations with a strong maximum of about $100\ \mathrm{m\ s^{-1}}$ at about 10 August and a minimum of about $-40\ \mathrm{m\ s^{-1}}$ at 28 September. This first reversal from westerlies to easterlies in the upper stratosphere down to 10 hPa indicates the major warming event (Fig. 1b) at the last week of September 2002. The second reverse at the end of October reflects the condition of the final warming before austral summer. Furthermore, three minor warming events (Fig. 1b) occurred around 25 August, 2

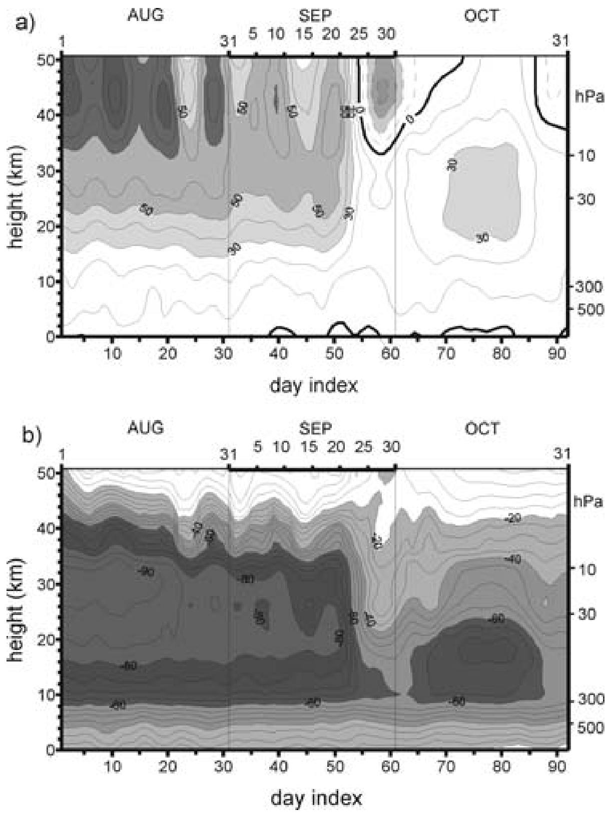

Fig. 1. Height-time cross section of (a) zonal mean zonal wind (m s^{-1}) at 65° S and of (b) temperature (° C) at 80° S during August, September and October 2002.

September and 15 September, which reduced the polar night jet (Fig. 1a).

Note, a similar evolution of the zonal mean zonal wind and temperature was shown by Baldwin et al. (2003) and Krüger et al. (2005) discussing the "pre-conditioning" of the major warming event.

To complete the short overview of the zonal mean evolution we show in Fig. 2 the E–P flux and its divergence of the quasi-stationary components for September 2002, and for comparison the same during the pre-warming and during the vortex splitting phase. In the pre-warming phase (Fig. 2b) an enlarged E–P flux occurs in the troposphere and lower stratosphere which is directed southward below 150 hPa in the extratropics. The strongest convergence at about 400 hPa between 50°S and 60°S, and the convergence over the whole region decelerate the zonal mean wind and improve the vertical propagation of shorter planetary waves (Charney and Drazin, 1961). During the splitting phase (Fig. 2c), we found an enlarged upward flux with strong convergences in the middle stratosphere of the extratropics. This E–P flux (or wave-activity flux) convergence is four times larger than the monthly mean one (Fig. 2a), and relates to the reverse of the zonal mean zonal wind in the middle and upper stratosphere (Fig. 1) and the sudden warming.

Furthermore, the amplitude evolution of planetary waves is shown in Fig. 3. The smoothed amplitudes (5 d running mean) for the waves 1–3 are averaged over 60–70° S, because in the climatological mean the amplitude maximum of planetary waves is observed about this latitudinal belt (Randel, 1987). At 30 hPa layer (Fig. 3a) the large oscillation of wave 1 dominates during the 3-month period. A strong increase was found until 25 August just in relation with the first minor warming, followed by a decrease of wave 1 and an increase of wave 2. During the second minor warming (2 September), both amplitudes are of similar magnitude. From the beginning of the first minor warming until the third minor warming at about day 15 of September the amplitudes of wave 1 and 2 are anti-correlated. This anti-correlation stops during the pre-warming and splitting phase, where both amplitudes are growing, and additionally, that of wave 3 with a time shift of some days. The decay of waves 2 and 3 starts 5 d earlier, about 25 September, than that of wave 1, about 30 September.

To study the tropospheric evolution of planetary waves we show in Fig. 3b the smoothed amplitudes of the 300 hPa layer. Note that we used a different scaling in Fig. 3b than in Fig. 3a. All amplitudes show an oscillating behaviour. Especially, we found a strong increase of wave 2 during the 12–17 September-period, just before the splitting period. Further on, wave 1 shows also a strong increase during the 15–20 September-period, but about 5 d later. At 500 hPa layer (not shown) the amplitudes evolution looks similar, indicating a strong wave 2 in the middle troposphere.

Krüger et al. (2005) found a dominating quasi-stationary wave 1 at 10 hPa in September with a weaker eastward traveling wave 2. However, they also estimated comparable heat fluxes at 100 hPa layer of wave 1 and 2 during the 16–30 September-period. The heat flux of wave 3 increases 5 d later than that of wave 1 and 2. They also showed the occurrence of a strong wave 2 at 500 hPa layer that is in agreement with our results of a strong wave 1 and 2 in the troposphere.

3.2. *Longitude dependent wave-activity flux*

For mid-latitudes, in Fig. 4a we show the mean wave disturbance of geopotential height and mean wave-activity flux averaged over the 45–55° S latitudinal belt for the 23 September. Strong tropospheric wave-activity fluxes are generated over the Southern Atlantic in the surrounding of the blocking high at about 10° W. The wave activity is propagating eastward and upward into the stratosphere between 0° E and 120° E. If the wave activity is conserved (no sources and no sinks) then a convergence of wave-activity flux cause a tendency to wave activity increase (P85). Consistent with that we could expect in regions of strong convergence a tendency of wave amplitude amplification and in regions of divergence a tendency of decrease.

In Fig. 4b the related convergence/ divergence of those fluxes are shown. In the stratosphere, the convergence at about 30° E

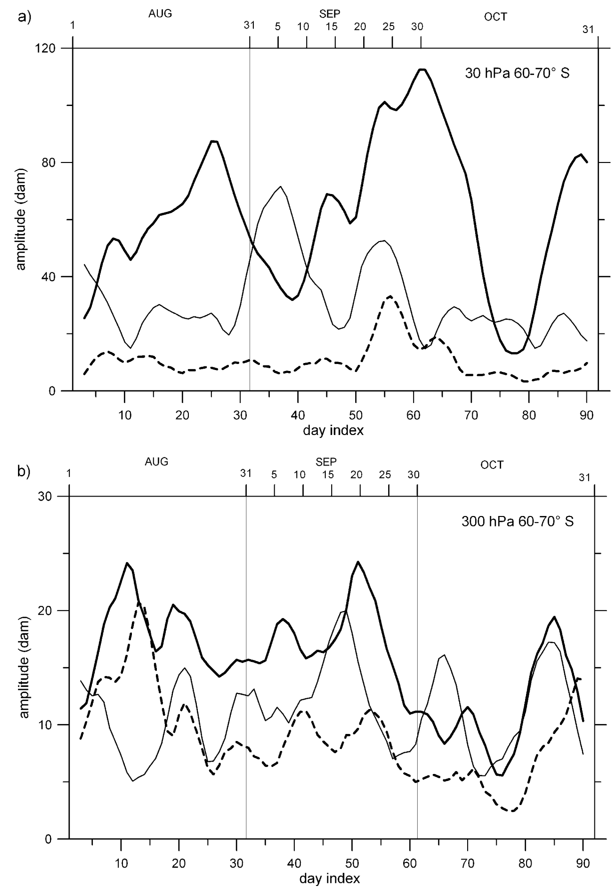

Fig. 3. The mean geopotential height amplitude evolution (dam) of planetary waves 1 (thick), 2 (thin) and 3 (dashed) is shown in (a) at 30 hPa and in (b) at 300 hPa layer averaged over a latitudinal band from 60° S to 70° S and using a 5 d running mean.

increases the cyclonic and that at about 80° E the anticyclonic structure on their westerly flank, but the divergence at about 60° E decreases the cyclonic structure on its easterly side. For mid-latitudes, our results confirm the finding of NN04. Furthermore, they found that strong tropospheric wave-activity fluxes appeared already 2 d earlier. This is also indicated in Fig. 5a for the 200 hPa layer on 21 September. We see strong wave-activity fluxes on the westerly flank of the blocking high between 20° W and 50° W at about 50° S. On the easterly side of it we see strong southward fluxes, which are directed to the cyclone

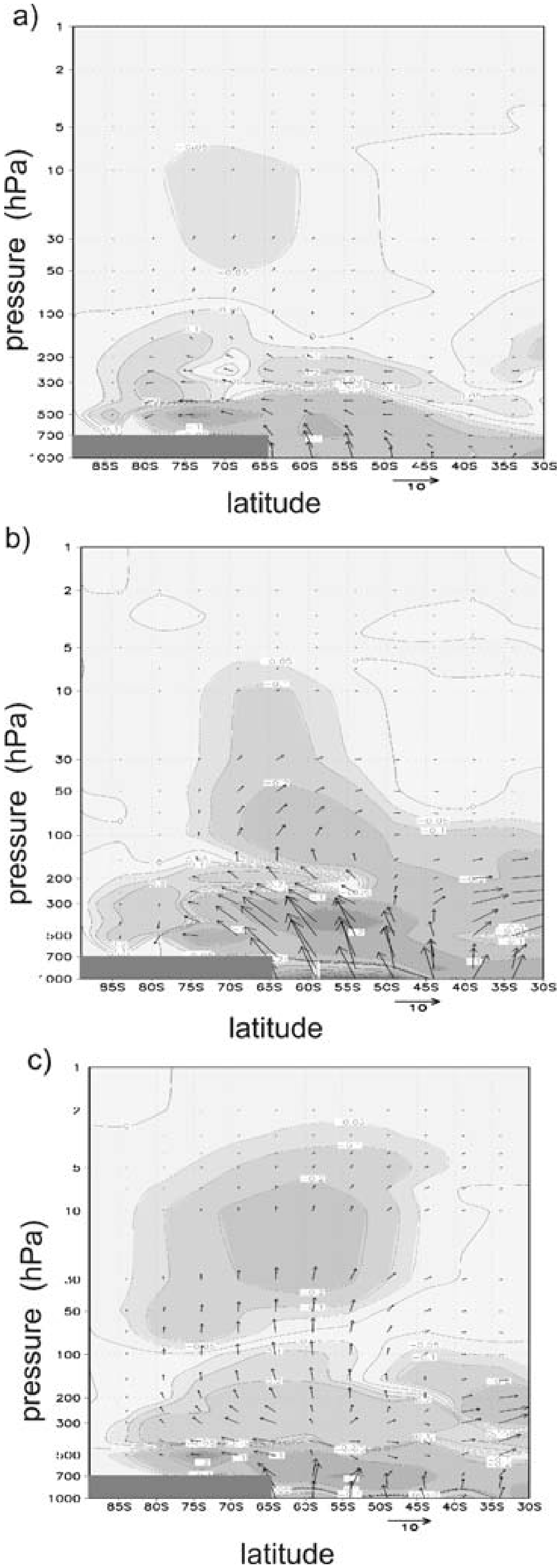

Fig. 2. Pressure-latitude cross-section of E–P flux (m^2 s^{-2}) for quasi-stationary waves: (a) averaged over September 2002, (b) averaged over 17–21 September-period and (c) over 23–27 September-period. Arrows indicate fluxes with a plotting factor of 100 for the vertical component, and contours indicate their divergences (10^{-5} m s^{-2}). Contours with negative values are dashed and shaded for amounts larger than 10^{-6} m s^{-2}. The black area indicates mean orography of Antarctica.

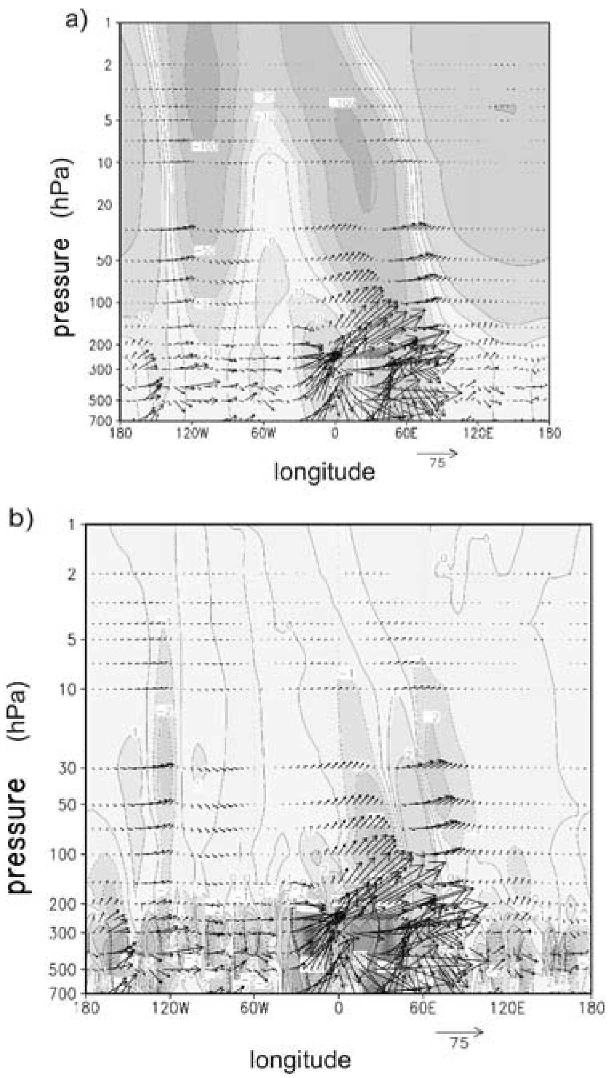

Fig. 4. Height-longitude cross-section of geopotential height disturbances and mean extended E–P flux (m^2 s^{-2}) with their divergences after Plumb (1985) averaged over a latitudinal belt from 45° S to 55° S for quasi-stationary waves: on 23 September 2002. Fluxes are indicated by arrows with a plotting factor of 100 for the vertical component; additionally in (b) their divergences (10^{-5} m s^{-2}) are plotted and in (a) the geopotential height deviation (dam) from zonal mean by contours. Contours with negative values are dashed.

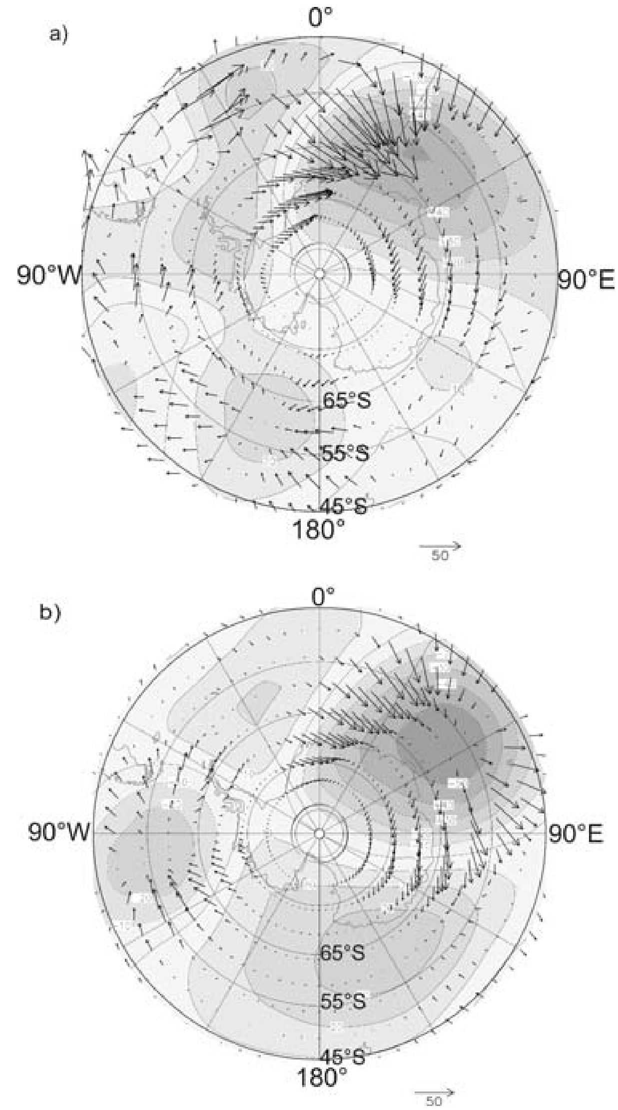

Fig. 5. Horizontal components of mean extended –E–P flux (m^2 s^{-2}) after Plumb (1985) for quasi-stationary waves: (a) at 200 hPa layer on 21 September, (b) at 150 hPa layer on 25 September 2002. Fluxes are indicated by arrows, and geopotential height deviation from zonal mean (dam) by contours, which are shaded.

centre at about (60° S, 40° E). Four days later at higher altitudes (150 hPa, Fig. 5b) we see also stronger eastward fluxes at about 90° E from the dominating cyclone to the largest anticyclone.

These results are in a good agreement with NN04 (their Fig. 2) supporting the hypothesis that in mid-latitudes tropospherically generated wave activity was propagating eastward and upward into the stratosphere by a Rossby wave packet (dominated by wave 1). These wave-activity fluxes amplified and maintained the vortex shift in the lower stratosphere during the major warming phase.

More southward (200 hPa, 21 September: Fig. 5a), the blocking high over the Atlantic extends southwestward in polar latitudes, and is weakened. A second similar strong tropospheric blocking high occurred over the South Central Pacific (53–70° S, 140–180° W) with comparable wave-activity fluxes on its westerly flank (150° E–160° W). Four days later and higher up (150 hPa, Fig. 5b) we see also strong eastward wave-activity fluxes (90–40° W) from the easterly side of the second weaker low to the second high.

In the following, we focus the investigation on polar latitudes especially on the latitudinal belt between 60° S and 70° S that means over the coastline of Antarctica, because we found in Fig. 5 indications for two polar centres of tropospherically generated wave activity.

In the whole troposphere (Fig. 6a), two main centres of strong eastward and upward wave-activity flux occur on 21 September, one on the easterly flank (180–150° W) of the Ross shelf ice and the other on the westerly side (120–60° W) of the Weddell shelf ice. In regions about 150–120° W and about 30° W–30° E, those fluxes enter the stratosphere whereby the fluxes in the last region dominate. Nevertheless, the first enter region about 150–120° W is related to a second but weak cyclonic disturbances in the upper troposphere and lower stratosphere. Additionally, in Fig. 6b we show the convergence and divergence for those wave-activity fluxes. In the stratosphere, the convergence at about 0° E increases the cyclonic and that at about 80° E the anticyclonic structure, but the divergence at about 60° E decreases the cyclonic structure. The structure and intensity for this polar belt is comparable with the mid-latitudinal structure over the eastern hemisphere 2 d later (Fig. 4b).

Two days later, on 23 September (Fig. 6c, d), the main tropospheric wave-activity generation regions are further intensified and shifted slightly eastward. Similarly, in both stratospheric enter regions the wave-activity fluxes show a strong increase, which cause an enlarged convergence over about 0–30° E, between about 90° E and 120° E, at about 120° W, and about 60° W and stronger divergences at about 60° E, 150° W, 90° W and 10° W. Again, we found dominating convergences and divergences over the eastern hemisphere. Obviously, this agrees well with the result of NN04, that a wave-1 was dominating, but over the western hemisphere similar strong convergences and divergences occurred linked to an increasing cyclonic disturbance over the westerly part of Antarctica.

Two days later (25 September, Fig. 6e and f) we found comparable wave-activity fluxes in the lower stratosphere eastward of both tropospheric generation regions, also the convergences and divergences are comparable. Both cyclonic disturbances in the stratosphere over westerly and easterly Antarctica are comparable strong and contribute to the ultra-long wave 2. This is in agreement with the amplitude evolution of ultra-long wave 2 given in Fig. 3b for 300 hPa. A separated calculation of convergences and divergences due to horizontal and vertical components of wave-activity flux vector shows that over the 180–100° W region, between 100 and 10 hPa layers, the horizontal flux contribution is larger than the vertical one (not shown). This was expected from the flux vector behaviour given in Fig. 6f, showing also the important role of incoming wave-activity flux carried by a quasi-stationary Rossby wave train from upstream in the stratosphere.

More generally, in addition to NN04, we found over the eastern side of the Ross shelf ice relatively strong convergences of wave activity (Fig. 6) which force the second cyclone at about 120° W. Again, on its western side, a blocking anticyclone occurred (Fig. 5a), which was related to the generation of lower tropospheric wave activity (Fig. 6). Therefore, as over the eastern hemisphere we found the same mechanism over the western hemisphere of Antarctica, which carried tropospherically generated wave activity into the stratosphere.

3.3. *Evolution of Rossby wave trains*

Over the South Atlantic Ocean, NN04 found a blocking anticyclone in mid-latitudes, which induced the enlarged wave-activity flux into the stratosphere during the pre-warming phase. In Fig. 5a we show that this anticyclone is stretched westwards and polewards with a second centre at about 75° W 65° S. In addition, at about 170° W we found a second tropospheric blocking anticyclone which induced also an enlarged wave-activity flux into the stratosphere (Fig. 3a–e). Transient Rossby waves (eddies) and quasi-stationary Rossby waves contribute to the maintenance of blocking anticyclones in the troposphere (Shutts, 1983, Nakamura and Wallace, 1990; Nakamura et al., 1997). We use the squared meridional wind component to examine if Rossby wave trains are linked with the observed anticyclones during the pre-splitting phase.

In Fig. 7 the Hovmöller diagram of the meridional velocity is shown at 300 hPa layer averaged over a latitudinal belt from 40° to 60° S during September 2002.

We identify two distinct wave trains in difference to NN04. The wave train starting at about 150–180° E, running over the South Pacific and South Atlantic, and ending at about 60–30° W is the one found by NN04. We found a second wave train to occur more westward which starts some days earlier at about 10–80° E, running over the Indian Ocean and South Pacific, and ending at about 150–120° W. Both Rossby wave trains are related to each of the anticyclonic blocking regions over the South Atlantic (with a westward shift of about 40°) and South Pacific in polar regions.

NN04 showed that the forcing region of the easterly Rossby wave train (Fig. 7) is well correlated with an outgoing long-wave radiation (for short OLR) anomaly in the tropics and subtropics especially with the convection over the northeast of Australia during the 13–17 September 2002. They conclude from their study that in a large cloud-covering region the vertical uplifting and divergence in the upper troposphere induces a relatively strong Rossby waves forcing.

For the westerly Rossby wave train (Fig. 7), we examine if a similar forcing mechanism can be identified. In Fig. 8 the evolution of interpolated OLR – NOAA anomaly from a climatology is presented averaged over three different areas capturing by 20–50° E and 10–40° S. During the 8–12 September 2002 relatively strong negative values occur, showing that over the above mentioned region, southeastward of South Africa (Agulhas stream region), increased cloud covering exists. In agreement with the proposed mechanism, in Fig. 9a we found a region of upward

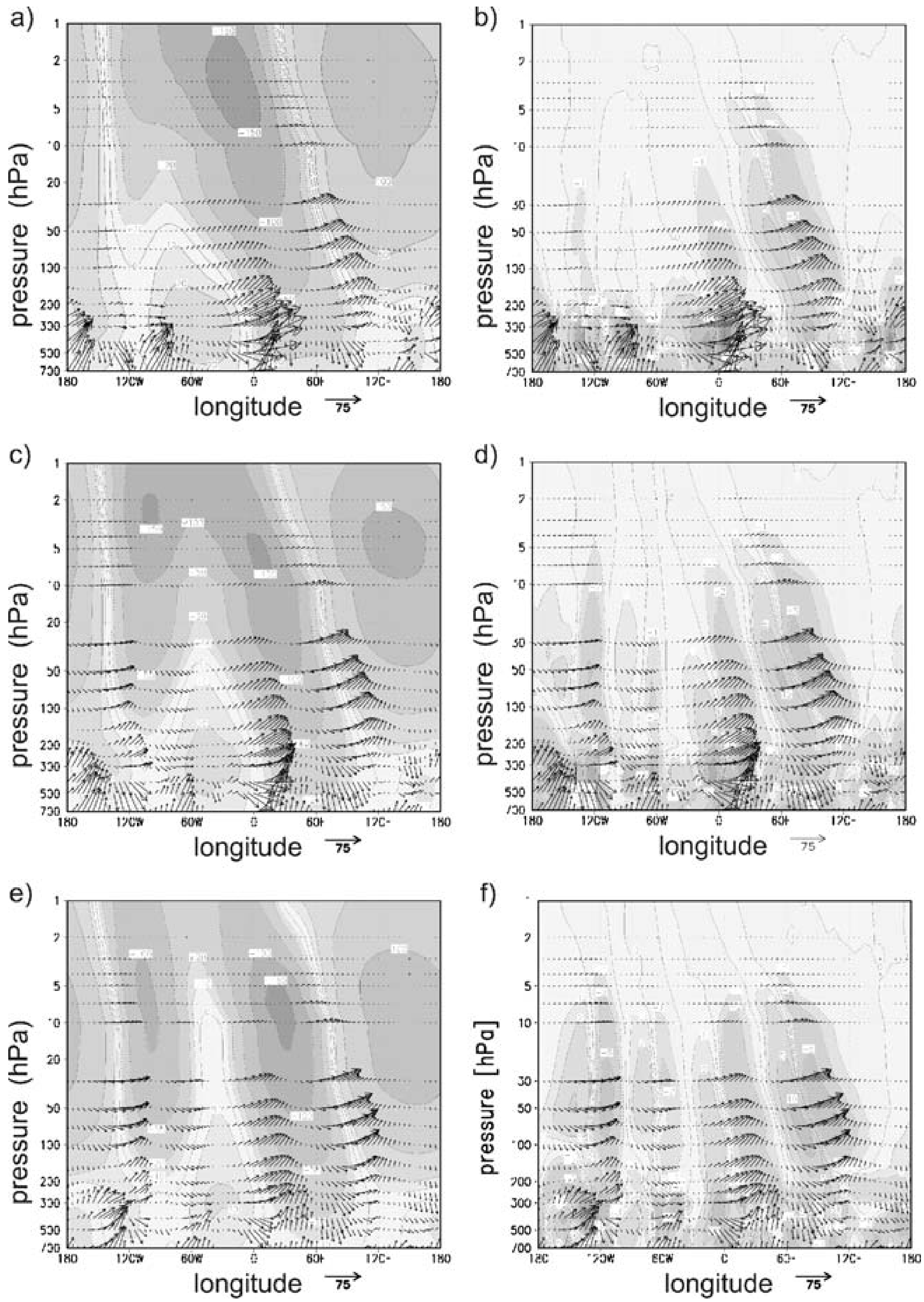

Fig. 6. Height-longitude cross section of geopotential height disturbances and mean extended E–P flux ($m^2 s^{-2}$) with their divergences after Plumb (1985) averaged over a latitudinal belt from 60 to 70° S for quasi-stationary waves: (a and b) on 21 September (c and d) on 23 September (e and f) on 25 September 2002. Fluxes are indicated by arrows with a plotting factor of 100 for the vertical component; additionally in (b, d and f) their divergences (10^{-5} m s^{-2}) are plotted and in (a, c and e) the geopotential height deviation (dam) from zonal mean by contours. Contours with negative values are dashed.

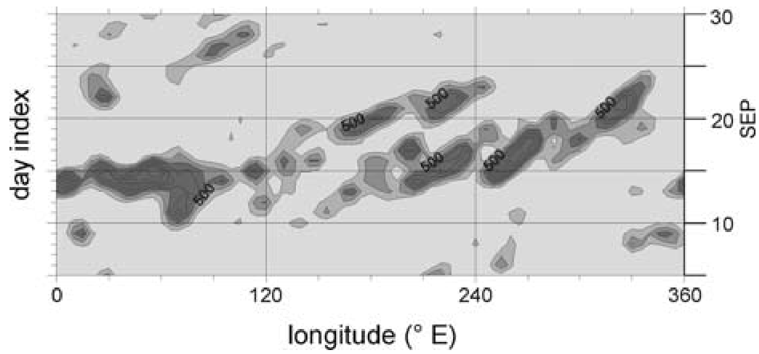

Fig. 7. Hovmöller diagram of the squared meridional wind component (m^2 s^{-2}) at 300 hPa layer averaged over a latitudinal band from 40° S to 60° S. Contours are smoothed with a Gauss filter and start at 300 m^2 s^{-2} with a step of 100 m^2 s^{-2}, and are shaded.

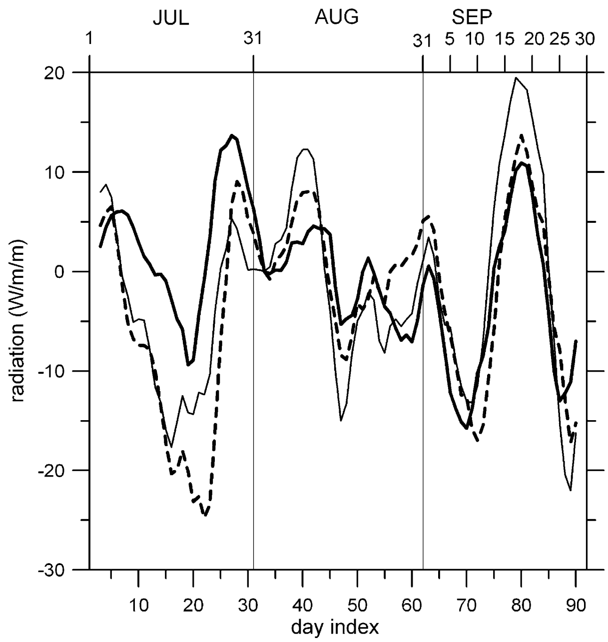

Fig. 8. Evolution of interpolated OLR-NOAA anomaly (W m^{-2}), deviation from climatology of 1979–2001 area averaged over {20–40° E; 10–30° S} thick line, {20–40° E; 20–40° S} thin line, and {30–50° E; 20–40° S} dashed line.

mean vertical velocity difference at about 300 hPa during 8–12 September 2002.

Further, we calculated the linear Rossby wave forcing as F = $-f\delta$ (Sardeshmukh and Hoskins, 1988), where f is the Coriolis parameter and δ the horizontal velocity divergence, for the monthly mean and for the 8–12 September period. The difference is plotted in Fig. 9b for the upper tropospheric layer about 300 hPa, showing an enhanced Rossby wave forcing in the same region where anomalies of the vertical velocity difference and of OLR occurred, namely over the Agulhas stream region. Therefore, we assume that a similar Rossby wave forcing mechanism is acting over the Agulhas stream region, due to convection processes warm and wet air masses are lifted upward into the tropopause region causing enlarged cloud covering and strong Rossby wave forcing by enlarged divergence as proposed by NN04 for the Indonesian region.

Rossby waves are propagating in the background stream and traveling over the Indian Ocean and South Pacific before reaching the anticyclonic blocking region. In Fig. 10a–c this propagation process is revealed by a one-point regression analysis using maps with time lags of {0; 2; 4 d} for a base point over the Agulhas stream region centred at 10 September with a 10 d overlapping interval. We found that the wave train from South Africa, over the Indian Ocean, and over the eastern South Pacific is already well established due to strong zonal winds (lag = 0; Fig. 10a). After 2 and 4 d the wave packets have been propagated relatively fast eastward over the Indian Ocean and South Pacific (about 30° per day). Note, the phase velocity is about 15° per day.

In addition, we calculated the one-point correlation maps for the Rossby wave forcing found by NN04 with a base point eastward of Australia that means 5 d later centred at 15 September (Fig. 10d–f). Obviously, for time lag = 0 the Rossby wave train is also well established over the Pacific and correlates to the earlier started wave train (Fig. 4c). The wave packets are propagating eastward for time lag = 2 and 4 d with a group velocity of about 30° per day into the anticyclonic blocking region over the South Atlantic.

4. Discussion

For the austral major warming event in September 2002, NN04 showed by wave-activity flux diagnostics that upward-propagating planetary waves originated mainly from a blocking ridge that developed over the South Atlantic in mid-latitudes. They also showed that the blocking formation was maintained by a Rossby wave train propagating over the South Pacific Ocean.

Our study based on ECMWF analysis 1° × 1° grid data set confirms the results found by NN04 for mid-latitudes. In difference to this study, NN04 used data of a reanalysis project by NCEP and NCAR with 2.5° intervals on a regular latitude–longitude grid.

In addition, we showed that more southwards in the 60–70° S latitudinal belt a similar mechanism was acting over the Weddell shelf ice region, however, the excitation of the Rossby wave

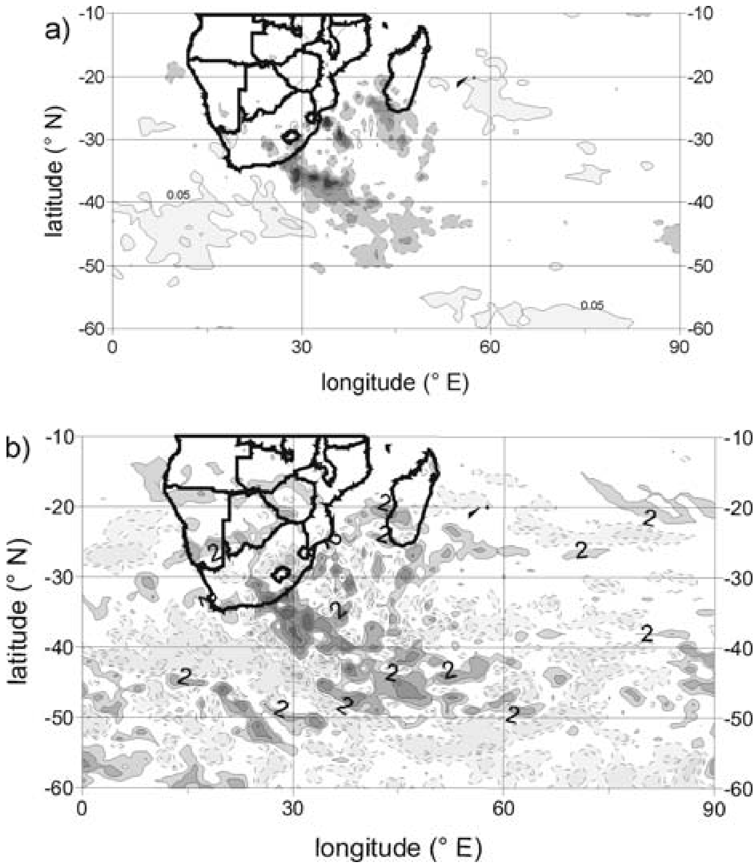

Fig. 9. Latitude–longitude cross section of (a) vertical velocity omega (Pa s^{-1}) and (b) Rossby wave source (10^{-10} s^{-2}) at level 34 (about 303 hPa) as difference: mean of 8–12 September 2000 minus monthly mean.

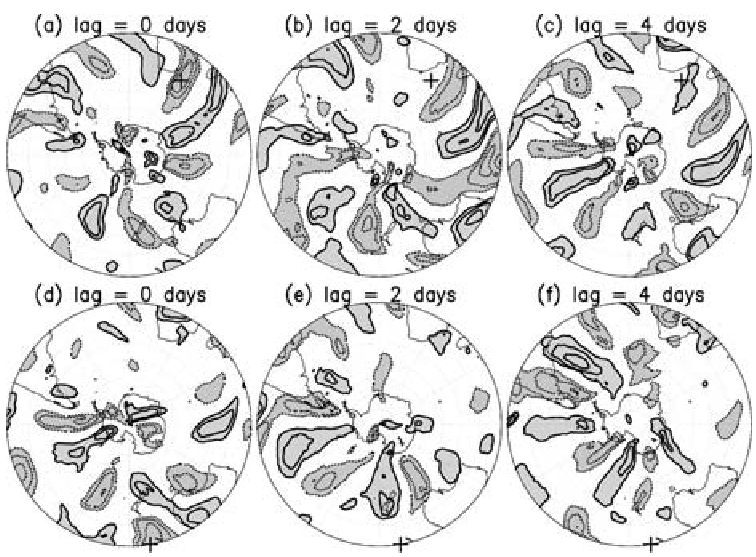

Fig. 10. One-point correlation map for meridional velocity at 300 hPa layer estimated over 10 d interval centred (a–c) at 10 September at base point 35° S, 35° E and (d–f) at 15 September 2002 at base point 20° S, 170° E with time lags up to 4 d. Contours start at an amount of 0.4 with a step of 0.2 with shading. Dashed lines indicate areas with negative correlations. A cross marks the base point.

train by convection over the Agulhas region was about 2 d earlier than that over the northeast of Australia. This was surprising, but shows that over the south-polar region wave-activity generation and propagation starts during the same time interval as the mid-latitudinal mechanism was activated. This wave-activity generation in the polar region is in agreement with results of Peters and Zülicke (2006) who estimated the component-evolution of atmospheric angular momentum balance for polar caps over Antarctica during September 2002, and showed a strong mountain torque generation in the pre-splitting phase.

Furthermore, we found over the eastern flank of the Ross shelf ice a relatively strong convergence of wave activity in the lower stratosphere, which forces a second cyclone over about 120° W. Again, on its western side, a tropospheric anticyclone occurs which is linked to the lower tropospheric wave-activity flux. Therefore, a comparable mechanism driven by tropospherically generated wave-activity fluxes cause the development of a second cyclone by strong convergences in the stratosphere of the western hemisphere. Both atmospheric regions of relatively strong wave-activity flux are found over regions with high orographic variability (western flank of Ross and Weddell shelf ice). That supports the hypothesis of topographic effects in the generation of wave activity. This is the subject of a future study and beyond the scope of this investigation.

We could show that a formation of an anticyclone was linked to a Rossby wave train starting over the Agulhas region about 10 September 2002, that means 5 d before the second Rossby wave train (identified by NN04) runs from the subtropical western Pacific to the South Atlantic. From idealized studies (Sardeshmukh and Hoskins, 1988) we know that in some specific basic streams Rossby wave trains could propagate eastward over the Indic Ocean and Pacific Ocean, if started over the top of South Africa. The second determined Rossby wave train, is the Pacific South America pattern known from climatological and model studies, too (Karoly, 1989, and Renwick and Revell, 1999). Due to our regression analysis we could show that both Rossby wave trains are observed in given basic streams in the pre-splitting phase during September 2002 and may have a link over the Pacific Ocean.

The above mentioned wave-activity forcing regions over the western flank of the Ross and Weddell shelf ice are directly linked to the evolution of the planetary waves in polar latitudes resulting in a relatively strong wave 2 component in the stratosphere. From our synoptic investigation, we conclude that lower tropospheric processes are primary responsible for initiating the vortex splitting.

Two main questions are not resolved in this study and wait for future considerations. Firstly, what determined the basic stream in September 2002, and secondly, what influenced the specified Rossby wave sources? Possible answers should be found in process studies of the interaction between subtropics and extratropics as done by Kodera and Yamada (2004) and Gray et al. (2005).

Further, some diagnostic papers showing that during the whole winter the large scale dynamics was characterized by strong vacillation processes between zonal mean flow and planetary waves (e.g. Scaife at al., 2005), and by anomalously strong —E–P fluxes (e.g. Harnik et al., 2005; Krüger et al., 2005; Newman and Nash, 2005). The pre-conditioning of the austral winter circulation seems to be relevant for the sudden warming. However, that is not a necessary condition for the splitting of the vortex. For instance, Kushner and Polvani (2005) showed with simple general circulation model simulations that such a major warming may be the result of a random process, rare but possible. However, further model simulations are necessary to examine the discussed mentioned mechanisms in more details, as well as the role of nonlinear ultra-long wave interaction process.

5. Conclusion

In the last week of September 2002, the first observed austral major warming was mainly characterized by a polar vortex splitting in the middle and upper stratosphere together with an ozone hole splitting. Based on ECMWF analyses, we examined tropospheric influences on the major warming and on the vortex splitting into two vortices.

For mid-latitudes we confirm results of NN04 using a different data set: A tropospheric anticyclone over the South Atlantic generates strong wave activity, which propagates upward and eastward by a wave packet of planetary waves. Through that mechanism, a dominant stratospheric cyclone–anticyclone structure (wave one) is enhanced and maintained during the major warming. A Rossby wave train starting southeastward of Indonesia some days earlier, contributes to the maintenance of the tropospheric anticyclone in the mid-latitudes, as was also shown by NN04.

In addition, for polar latitudes, we found two regions over the coastline of Antarctica, one over the eastern flank of the Ross shelf ice and the other over western side of the Weddell shelf ice, where an enlarged tropospheric wave-activity generation in connection with two anticyclones took place. The wave-activities at both regions propagate eastward and upward into the stratosphere. They contribute to the intensification and maintenance of two stratospheric cyclones (wave 2 component) during the major warming. Further, in the troposphere, two different Rossby wave trains have been identified which contribute to the maintenance of those anticyclones related to both wave-activity generation regions.

We established the hypothesis that in the austral polar region the tropospheric generation of wave activity at two different regions has a strong influence on the vortex splitting in September 2002. However, model simulations are necessary to examine the mentioned mechanism in more details.

Acknowledgments

The authors thank the Deutscher Wetterdienst and ECMWF in Reading for providing the ECMWF analyses. Interpolated OLR data gratefully provided by the NOAA-CIRES Climate Diagnostics Center, Boulder, Colorado, USA, are from their Web site at http://www.cdc.noaa.gov/. We thankfully acknowledge the help of Frau H. Voss in calculating wave fluxes and Ch. Zülicke for data processing of ECMWF analyses. We thank G. Schmitz for fruitful discussions. One of us, P. Vargin, wants to thank the German Science Foundation for the support of his work at the Leibniz-Institute of Atmospheric Physics.

References

Allen, D. R., Bevilacqua, R. M., and Nedoluha, G. E. 2003. Unusual stratospheric transport and mixing during the 2002 Antarctic. *Geophys. Res. Lett.* **30**, doi:10.1029/2003GL017117.

Chang, E. K. M. 1993. Downstream development of Baroclinic waves as inferred from regression analysis. *J. Atmos. Sci.* **50**,2038–2053.

Charlton, A. J., O´Neill, A., Lahoz, W. A., and Berrisford, P. 2005. The splitting of the stratospheric polar vortex in the southern hemisphere, September 2002: Dynamical evolution. *J. Atmos. Sci.* **62**, 590–602.

Charney, J. and Drazin, P. G. 1961. Propagation of planetary-scale disturbances from the lower in to the upper atmosphere. *J. Geophus. Res.* **66**, 83–109.

Baldwin, M., Hirooka, T., O´Neill, A., and Yoden, S. 2003. Major stratospheric warming in the southern hemisphere in 2002: dynamical aspects of the ozone hole split. *SPARC Newsletter No.* **20**, 24–26.

Bretherton, C. S., Smith, C. S., and Wallace, J. M. 1992. An intercomparison of methods for finding coupled patterns in climate data. *J. Climate* **5**, 541–560.

Gray, L., Norton, W., Pascoe, Ch., and Charlton, A. 2005. A possible influence of equatorial winds on the September 2002 southern hemisphere sudden warming event. *J. Atmos. Sci.* **62**, 651–667.

Harnik, N., Scott, R. K., and Perlwitz, J. 2005. Wave Reflection and Focusing prior to the Major Stratospheric Warming of September 2002. *J. Atmos. Sci.* **62**, 640–650.

Karoly, D. J. 1989. Southern hemisphere circulation features associated with El Nino-Southern oscillation events. *J. Climate* **2**, 1239–1251.

Kodera, K. and Yamada, K. 2004. Impact of the SH major stratospheric warming on the Hadley circulation: A case study. *Meteorol Geophys* **54**, 111–116.

Krüger, K., Naujokat, B., and Labitzke, K. 2005. The Unusual Midwinter Warming in the Southern Hemisphere Stratosphere 2002: A Comparison to Northern Hemisphere Phenomena. *J. Atmos. Sci.* **62**, 603–613.

Kushner, P. J. and Polvani, L. M. 2005. Avery large, spontaneous stratospheric sudden warming in a simple AGCM: A prototype for the southern hemisphere warming of 2002? *J. Atmos. Sci.* **62**, 890–897.

Labitzke, K. and Naujokat, B. 2000. The lower Arctic stratosphere in winter since 1952. *SPARC Newslett.*, No. 15, SPARC Office, Toronto, ON, Canada, 11–14.

Manney, G. L., Sabutis, J. L., Allen, D. R., Lahoz, W. A., Scaife, A. A., and co-authors. 2005. Simulations of dynamics and transport during the September 2002 Antarctic major warming. *J. Atmos. Sci.* **62**, 690–707.

Matsuno, T. 1971.A dynamical model of stratospheric sudden warming. *J. Atmos. Sci.* **28**, 1479–1494.

Nakamura, H. and Wallace, J. M. 1990. Observed changes in baroclinic wave activity during the life cycles of low-frequncy circulation anomalies, *J. Atmos. Sci.* **47**, 1100–1116.

Nakamura, H., Nakamura, M., and Anderson, J. L. 1997. The role of high- and low-frequency dynamics in blocking formation, *Mon. Weather Rev.* **125**, 2074–2093.

Newmann, P. A. and Nash, E. R. 2005. The Unusual Southern Hemisphere Stratosphere Winter of 2002. *J. Atmos. Sci.* **62**, 614–628.

Nishii, K. and Nakamura, H. 2004. Tropospheric influence on the diminished Antarctic ozone hole in September 2002, *Geophys. Res. Lett.* **31**, doi:10,1029/2004GL019532.

Orsolini, Y. J., Randall, C. E., Manney, G. L., and Allen, D. R. 2005. An Observational Study of the Final Breakdown of the Southern Hemisphere Stratosphere Vortex in 2002. *J. Atmos. Sci.* **62**, 735–747.

Peters, D. and Zülicke, Ch. 2006. Atmospheric angular momentum balance for the southern hemisphere during the polar vortex break-up of September 2002. *Tellus* **58A**, 508–519, doi: 10.1111/j.1600-0870.2006.00187.x.

Plumb, R. A. 1981. Instability of the disturbed polar night vortex: A theory pf stratospheric warmings. *J. Atmos. Sci.* **38**, 2514–2531.

Plumb, R. A. 1985. On the Three-Dimensional Propagation of Stationary Waves. *J. Atmos. Sci.* **42**, 217–229.

Randel, W.J. 1987. Global atmospheric circulation statistics 1000-1 mb. *NCAR Technical Note, NCAR/TN-295+STR*, 255pp., Boulder, Colorado.

Renwick, J. A. and Revell, M. J. 1999. Blocking over the South Pacific and Rossby wave propagation. *Mon. Wea. Rev.* **127**, 2233–2247.

Sardeshmukh, P. D. and Hoskins, B. J. 1988. The generation of global rotational flow by steady idealized tropical divergence. *J.Atmos. Sci.* **45**, 1228–1250.

Scaife, A. A., Jackson, D. R., Swinbank, R., Butchart, N., Thornton, H. E., and co-authors. 2005. Stratospheric Vacillations and Major Warming over Antarctica in 2002. *J. Atmos. Sci.* **62**, 629–639.

Scherhag, R. 1952. Die explosionsartigen Stratosphärenerwärmungen des Spätwinters 1951/52. *Berichte des Deutschen Wetterdienstes in der US-Zone* **6(Nr. 38)**, 51–63.

Shutts, G. J. 1983. The propagation of eddies in different jet streams: Eddy vorticity forcing of blocking flow fields. *Quart. J. Roy. Meteor. Soc.* **109**, 737–761.

Simmons, A., Hortal, M., Kelly, G. McNally, A., Untch, A., and co-authors. 2003. Analyses and forecasts of stratospheric winter polar vortex break-up: September 2002 in the southern hemisphere and related events from ECMWF operations and ERA-40. *ERA-40 project report series no.* **5** The Library ECMWF, Reading, 28 pp.